DEVELOPMENTAL DYNAMICS 210:431–445 (1997)

Genetic Patterning of the Developing Mouse Tail at the Time of Posterior Neuropore Closure

F. GOFFLOT, M. HALL, AND G.M. MORRISS-KAY*
Department of Human Anatomy, University of Oxford, Oxford, United Kingdom

ABSTRACT **Posterior neuropore (PNP) closure coincides with the end of gastrulation, marking the end of primary neurulation and primary body axis formation. Secondary neurulation and axis formation involve differentiation of the tail bud mesenchyme. Genetic control of the primary-secondary transition is not understood. We report a detailed analysis of gene expression in the caudal region of day 10 mouse embryos during primary neuropore closure. Embryos were collected at the 27–32 somite stage, fixed, processed for whole mount in situ hybridisation, and subsequently sectioned for a more detailed analysis. Genes selected for study include those involved in the key events of gastrulation and neurulation at earlier stages and more cranial levels. Patterns of expression within the tail bud, neural plate, recently closed neural tube, notochord, hindgut, mesoderm, and surface ectoderm are illustrated and described. Specifically, we report continuity of expression of the genes *Wnt5a*, *Wnt5b*, *Evx1*, *Fgf8*, *RARγ*, *Brachyury*, and *Hoxb1* from primitive streak and node into subpopulations of the tail bud and caudal axial structures. Within the caudal notochord, developing floorplate, and hindgut, *HNF3α*, *HNF3β*, *Shh*, and *Brachyury* expression domains correlate directly with known genetic roles and predicted tissue interdependence during induction and differentiation of these structures. The patterns of expression of *Wnt5a*, *Hoxb1*, *Brachyury*, *RARγ*, and *Evx1*, together with observations on proliferation, reveal that the caudal mesoderm is organised at a molecular level into distinct domains delineated by longitudinal and transverse borders before histological differentiation. Expression of *Wnt5a* in the ventral ectodermal ridge supports previous evidence that this structure is involved in epithelial-mesenchymal interaction. These results provide a foundation for understanding the mechanisms facilitating transition from primary to secondary body axis formation, as well as the factors involved in defective spinal neurulation.** ***Dev. Dyn. 1997;210:431–445.*** **© 1997 Wiley-Liss, Inc.**

Key words: neurulation; gastrulation; gene expression; posterior neuropore; mouse embryo; cell proliferation; in situ hybridisation

INTRODUCTION

In amniote embryos, the neural tube is formed by two different processes. During primary neurulation, the neuroepithelium differentiates directly from the epiblast in a craniocaudal sequence, followed by morphogenesis to form the neural tube and neural crest. At the future lumbosacral region of the embryo, this process ends abruptly with closure of the posterior neuropore (PNP) at approximately the 28–30 somite stage in mouse and human embryos, to be succeeded by a quite different mechanism. Tail bud mesenchyme, a tissue formed during the final phase of gastrulation, condenses to form a cord of cells that becomes canalised, so that neuroepithelial differentiation and neural tube formation are simultaneous. This developmentally significant change from primary to secondary neurulation coincides with the end of gastrulation. The notochord and somites, which until this stage are derived directly from cells that have undergone gastrulation through the node and primitive streak, respectively (Lawson et al., 1991; Wilson and Beddington, 1996), henceforth differentiate from the stem cell-like population of the tail bud mesenchyme. Cell labelling studies suggest that there is a continuity between the two modes of axis formation in that the tail bud cells have their origin in cell populations within the primitive streak and node (Wilson and Beddington, 1996), but the transformation is nevertheless remarkable.

At the axial level at which these changes take place, there are significant discontinuities in the gut and the vascular system. During primary neurulation, the blind-ended hindgut extends with the extending axis; it ceases to do so after PNP closure, extending only a short distance into the elongating tail bud. Similarly, the dorsal aortae loop ventrally and cranially at the caudal end of the gut, joining ventrally to form the omphalomesenteric vein, whereas the more caudal vasculature is formed from angiogenetic sprouts from these vessels (Wood et al., 1997).

Although the normal result of this change from primary to secondary axis formation is seamless conti-

Grant sponsor: Medical Research Council; Grant number: G9421750N; Grant sponsor: European Molecular Biology Organisation; Grant sponsor: Foulkes Foundation.

F. Gofflot's current address is Laboratory of Developmental Genetics, Catholic University of Louvain-la-Neuve, 1348-Louvain-la-Neuve, Belgium.

*Correspondence to: Professor Gillian M. Morriss-Kay, Department of Human Anatomy, South Parks Road, Oxford OX1 3QX, United Kingdom.

Received 14 July 1997; Accepted 30 August 1997

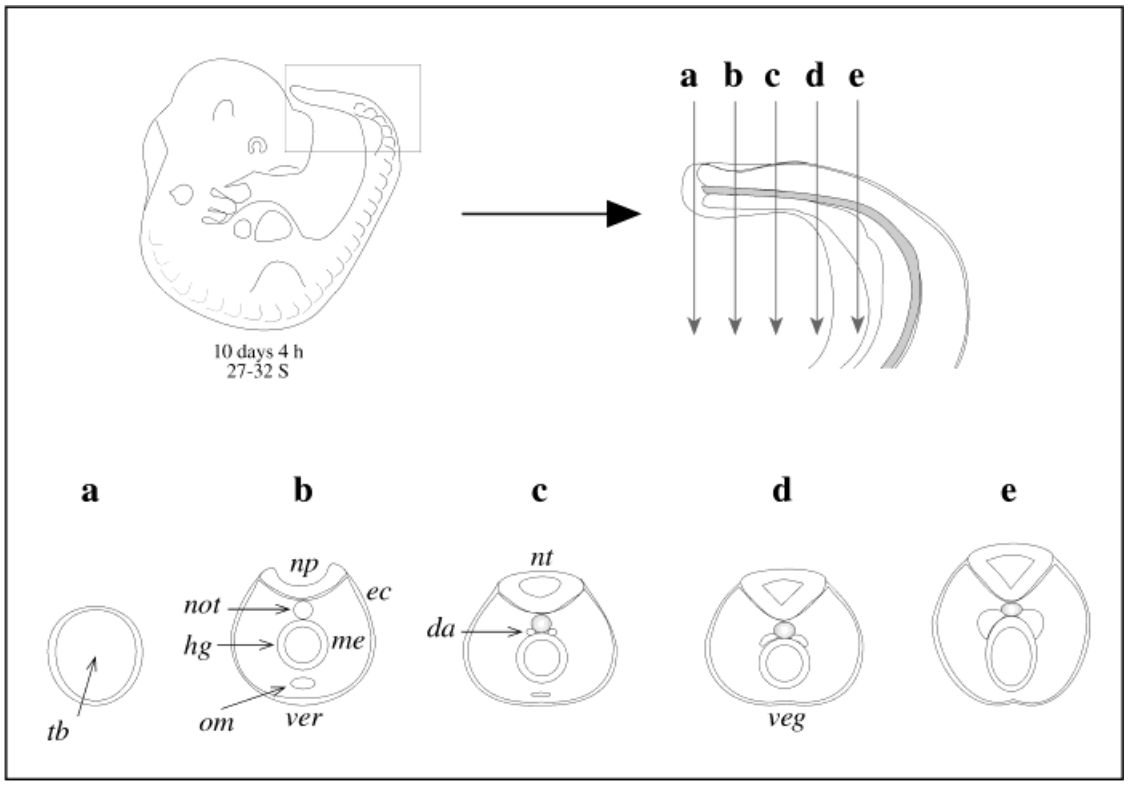

Fig. 1. Schematic drawings of the procedure for preparation and analysis of embryonic tails by whole mount in situ hybridisation followed by vibratome sectioning. Five levels of section (a–e), selected at equal distances from caudal to cranial, were used for illustration and quantitative cell proliferation analysis. da, dorsal aorta; ec, ectoderm; hg, hindgut; me, mesenchyme; not, notochord; np, neural plate; nt, neural tube; om, omphalomesenteric artery; tb, tail bud; ver, ventral ectodermal ridge; veg, ventral ectodermal groove.

nuity in the formation of the neural tube, notochord, and segmental structures, the point of change is particularly vulnerable to developmental abnormalities. These include open neural tube defects (lumbosacral spina bifida), abnormalities of the lumbosacral vertebrae, and tail flexures. An open neural tube clearly results from failure of primary neurulation to continue to the point of change to secondary neurulation, but the reasons for this failure are not understood. Development of all the tissues of this region of the embryo is intimately integrated, and deviation from the ideal developmental programme in any one of them will have consequences for one or more of the others.

Gastrulation and neurulation depend on coordinated expression of regulatory genes, encoding either transcription factors or secreted signalling molecules, whose effects influence cell proliferation, cell movement, and differentiation (reviewed by Faust and Magnuson, 1993). During primary neurulation, *RAR*β is expressed in the closed neural tube and *RAR*γ is expressed in the open PNP and caudal mesenchyme (Ruberte et al., 1991). The notochord is involved in neuroepithelial differentiation and patterning (see Placzek, 1995, for review); its own differentiation requires *HNF3*β, acting upstream of *Brachyury* and *Shh* (Ang and Rossant, 1994; Hermann, 1995; Chiang et al., 1996). Early induction of mesodermal cells involves members of the Fgf and Wnt families (reviewed by Parr and McMahon, 1994; Yamaguchi and Rossant, 1995). Downstream of these genes, *Evx1*, a homeobox gene, and *Brachyury* have been implicated in specification of the different subtypes of mesoderm (Dush and Martin, 1992; Hermann, 1995). *Hoxb1* is another member of the homeobox gene family expressed within the primitive streak in the newly formed mesoderm (Murphy and Hill, 1991). Most of the endoderm present in the central core of the tail is formed as an early event during gastrulation, probably under control of a member of the *HNF* family, and evolved as an independent lineage (Lawson et al., 1991; Ang et al., 1993). At the tip of the tail, the remnants of the primitive streak and node form the tail bud caudal to the closing neuropore. Cells of the tail bud express many of the genes previously present in the posterior streak, and no genes specific to tail bud cells have yet been reported. The surface epithelium of the tail derives from the caudal extremity of the epiblast. On the ventral surface of the tail, the surface ectoderm thickens to form the ventral ectodermal ridge (VER), continuous cranially with the ventral ectodermal groove (VEG) and ending at the level of the cloacal membrane (Gajovic and Kostovic-Knezevic, 1995). The developmental

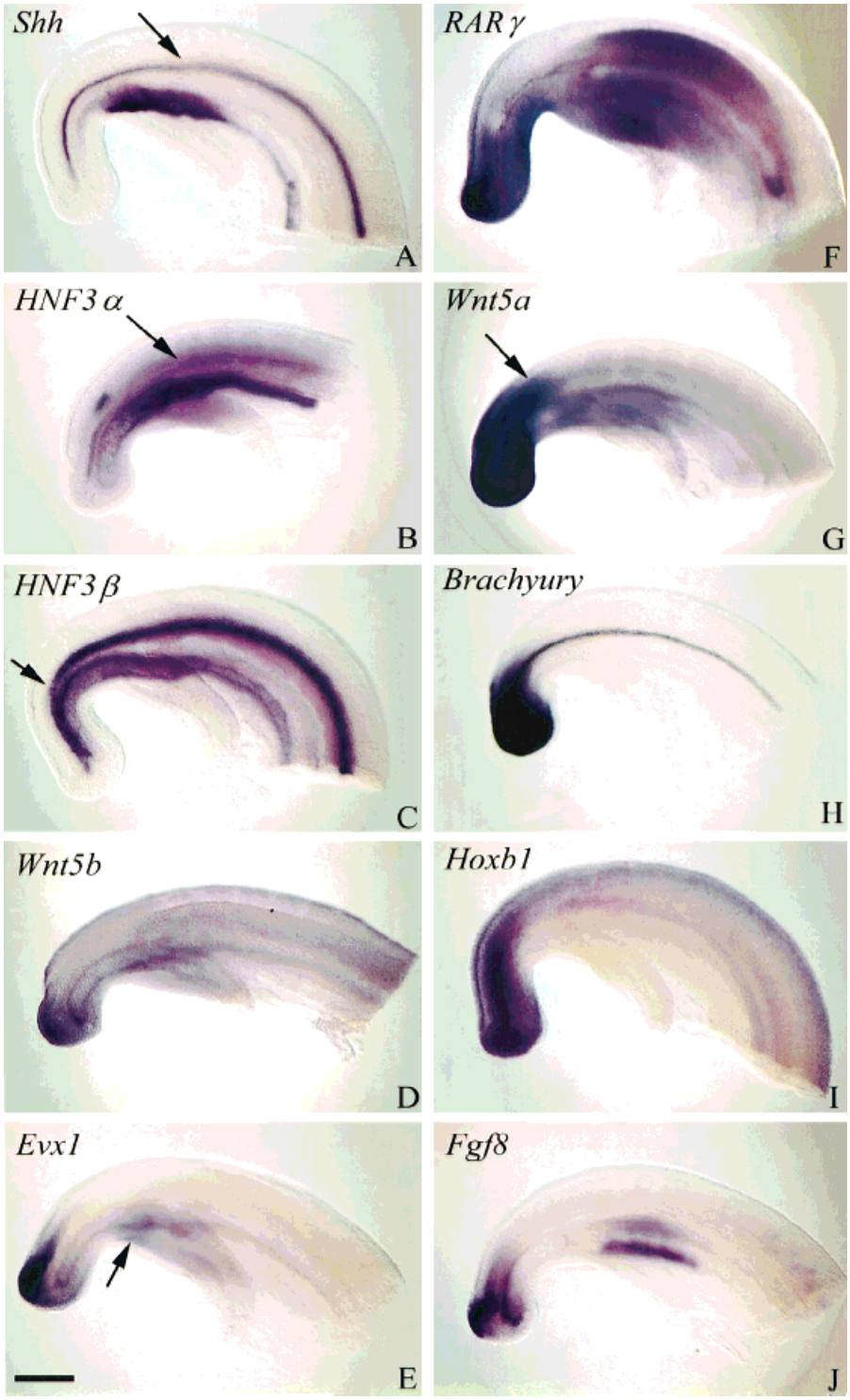

Fig. 2. Whole mount in situ hybridisation of day 10 embryos (28–30 somite stage) revealing expression of the genes indicated. (**A–C**) Transcripts are present in the hindgut and cloaca ventrally, the notochord, and the ventral part of the neural tube. Arrows indicate the caudal border of expression in the floorplate. (**D**) Expression of *Wnt5b* is restricted to a very small domain at the caudal end of the tail, including the tip of the hindgut. (**E**) The ventral expression domain (arrow) is in the mesoderm cranial to the ventral curvature. (**F–J**) These five genes show a high level of expression in the tail bud and the area just adjacent to it, with a border of expression located near the level of the ventral curvature. Cranial to this, *RAR-γ* is expressed mainly in the limb buds, *Brachyury* only in the notochord, *Hoxb1* mainly in the dorsal neural tube, and *Fgf8* in the developing apical ectodermal ridge of the hindlimb buds as well as the adjacent flank mesenchyme. The arrow in G indicates a high level of expression in the condensing somite. Scale bar = 1 mm

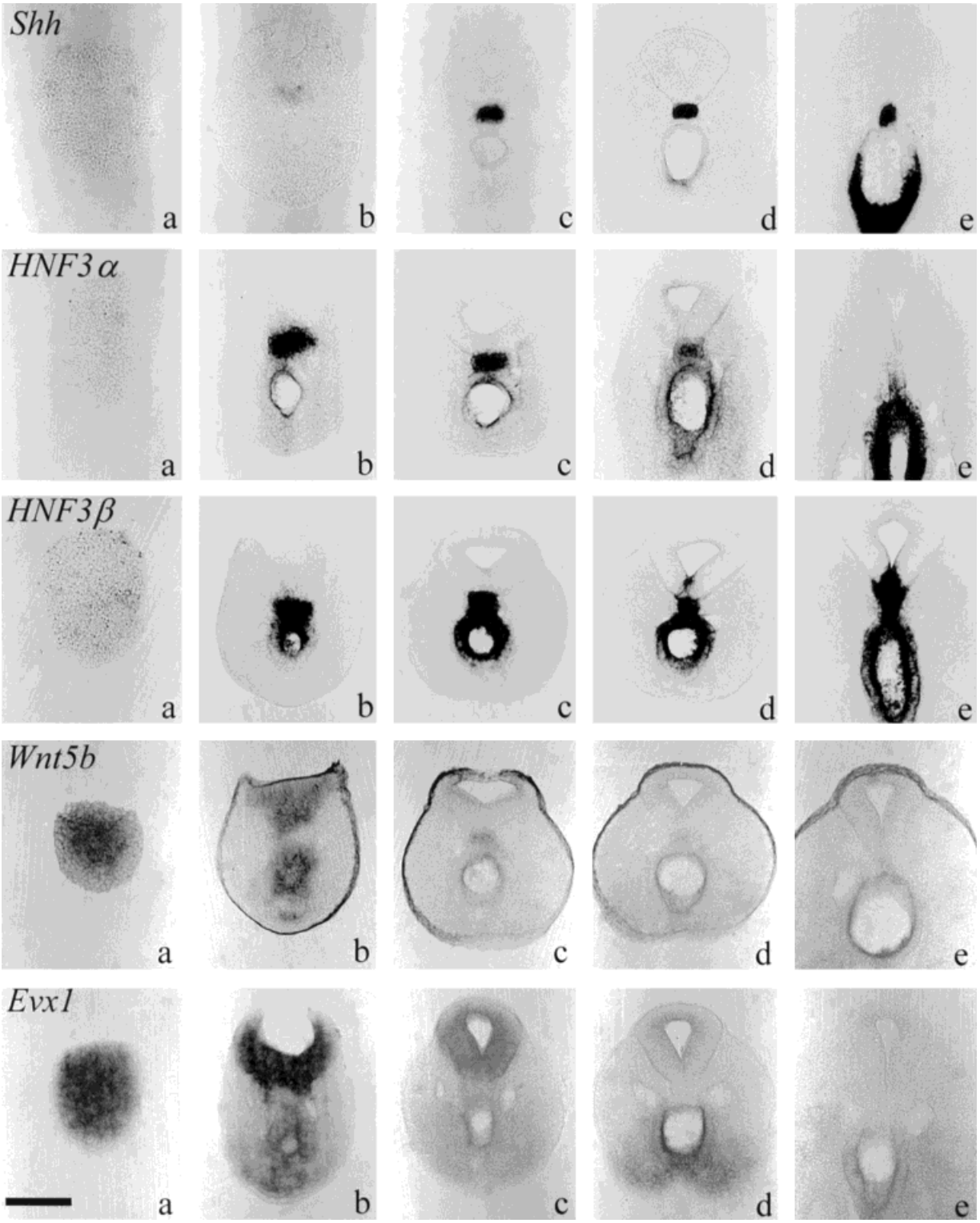

Fig. 3. Transverse vibratome sections (50 µm) of tails hybridised with probes for the genes indicated. Sections are presented in a caudal to cranial sequence (**a–e**), with each section being 150 µm cranial to the previous one. Scale bar = 500 µm

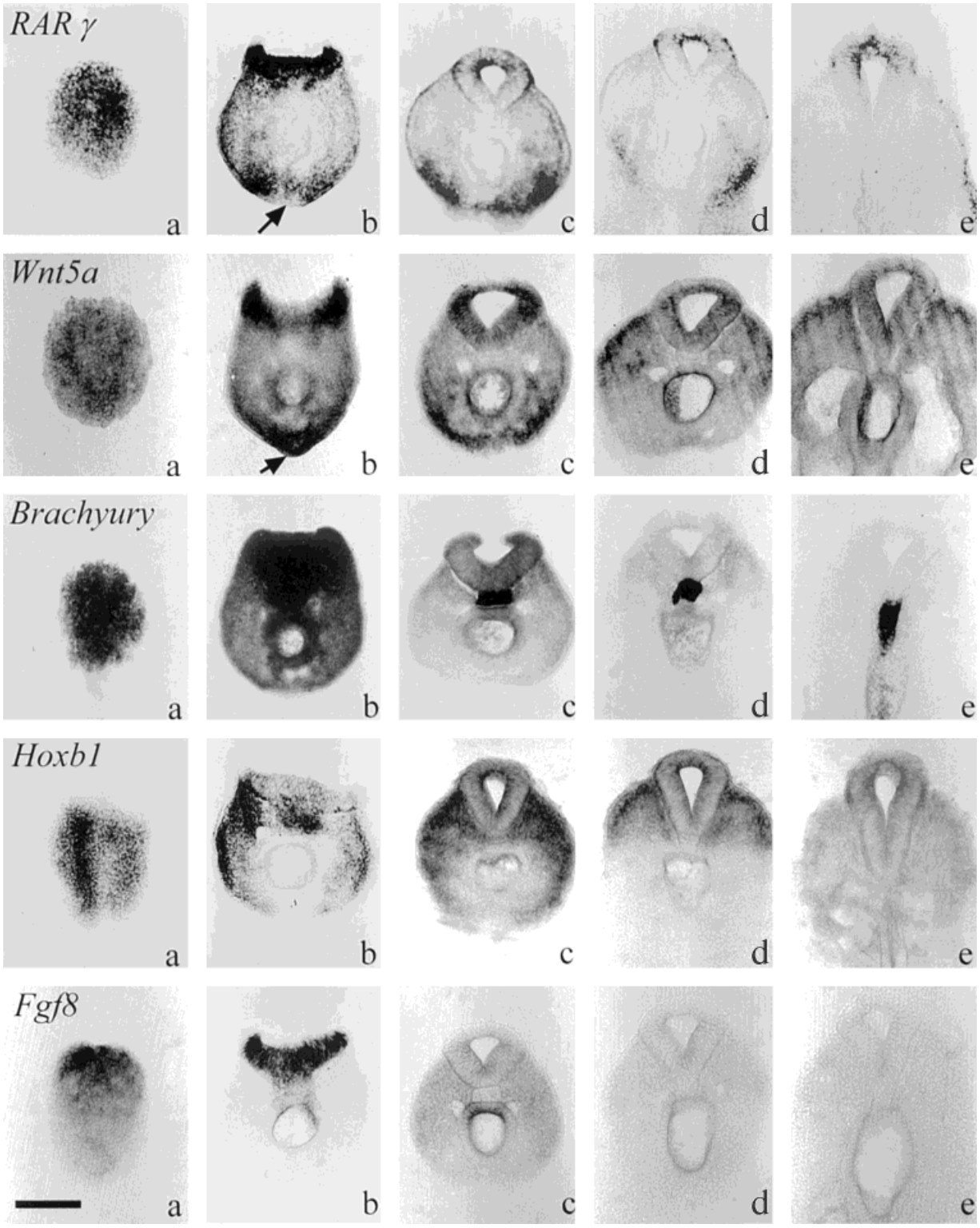

Fig. 3. (Continued)

significance of these epithelial specialisations is unknown.

The closure of the PNP marks the conclusion of two key embryonic events in the mouse, gastrulation and primary neurulation. Despite our current understanding of tail morphogenesis as outlined above and of gene expression during earlier stages of gastrulation and neurulation, little is known of genetic patterning and

Fig. 4. Diagrams of serial transverse sections through the tail of day 10 mouse embryos summarising the patterns of expression of the genes indicated, based on three to nine specimens for each gene. Different levels of transcripts are represented by different levels of gray.

the potential morphogenetic role of regulatory molecules in the mouse tail in relation to PNP closure. This study aims to fill this gap in the descriptive literature through a detailed analysis of gene expression in the embryonic mouse tail during PNP closure. Genes selected include those involved in the key events of gastrulation and neurulation at earlier stages and more cranial levels: *Shh, HNF3*α, *HNF3*β, *Wnt5b, Evx1, RAR*γ, *Hoxb1, Brachyury, Wnt5a,* and *Fgf8*. To correlate these results more closely with morphogenetic events in the developing tail region, a cell proliferation analysis was also performed. The results show some significant continuities of gene expression between regions of primary and secondary axial development and some correlations between cell proliferation and gene expression domains in the caudal mesenchyme.

RESULTS

Patterns of Gene Expression

Patterns of gene expression were initially studied on whole embryos after in situ hybridisation. To facilitate analysis, tails were isolated from the embryos by a cut

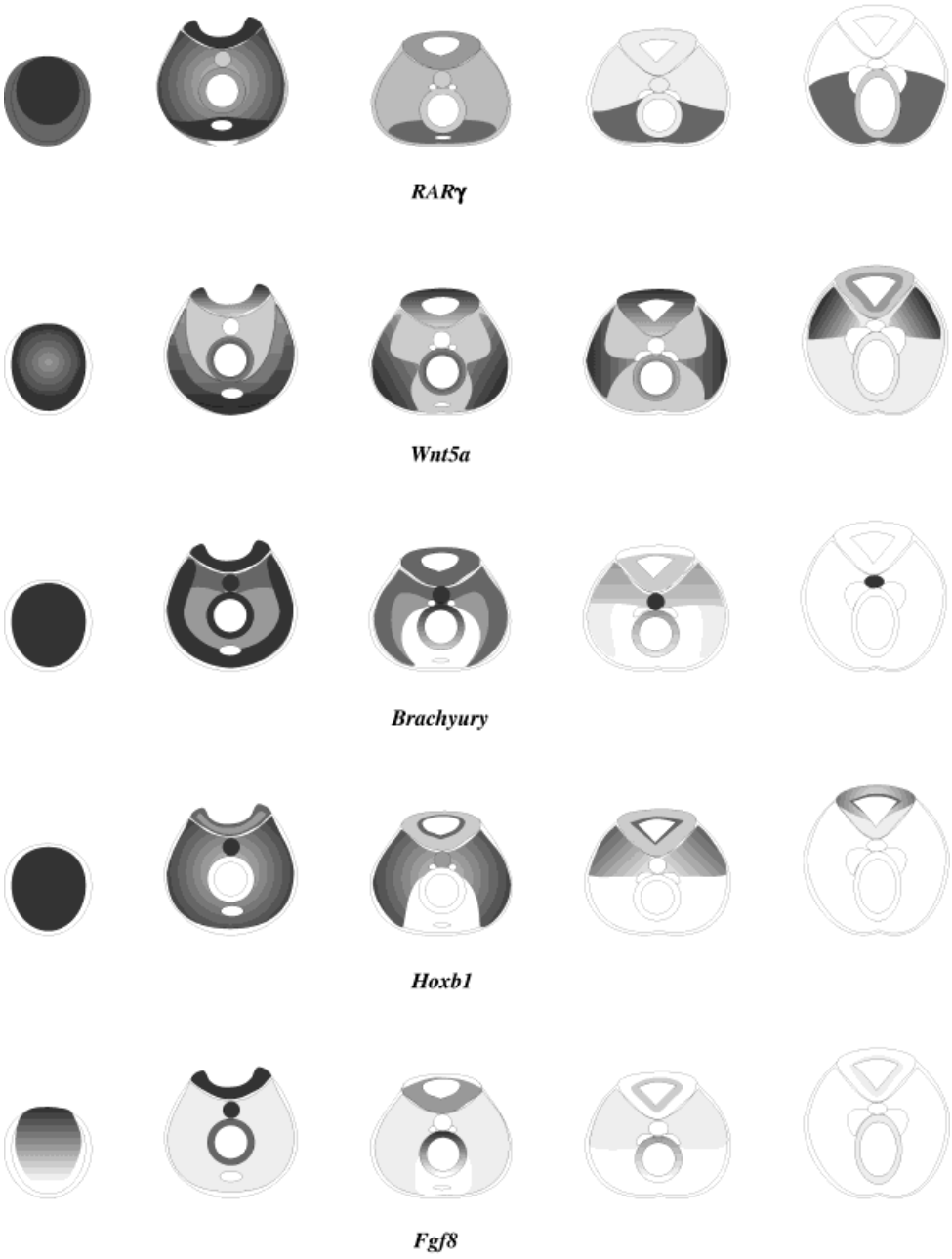

Fig. 4. (Continued)

just cranial to the hindlimb buds (Fig. 1). At least nine embryos were hybridised with each probe. Subsequently, vibratome sections of the tails were made. Between 3 and 13 embryos were sectioned for each gene. Patterns of gene expression are described for the 10 genes, with reference to photographic illustrations (Figs. 2, 3) and summary drawings (Fig. 4). The description focuses on the PNP region and tail bud, because expression patterns of the selected genes in other developing embryonic structures are available elsewhere (Gavin et al., 1990; Murphy and Hill, 1991; Ruberte et al., 1991; Dush and Martin, 1992; Ang et al., 1993; Echelard et al., 1993; Hermann, 1995; Mahmood et al., 1995). The following descriptions refer to whole isolated tails and to serial sections, of which five levels have been selected for illustration. Because development proceeds in a cranial to caudal sequence in the neural and mesodermal tissues, sections from the tail bud to more cranial levels represent progressively more mature stages of these tissues. Apart from the tail bud, five distinct tissues can be recognized morphologically at the stage of development studied here (Fig. 1): the

neural plate/folds/tube, present dorsally; the notochord, immediately ventral to the neural tissue; the dilated cloacal region of the hindgut; the surrounding mesenchyme; and the surface ectoderm, with its ventral midline features, VER and VEG.

Shh. Shh expression is detected along the whole length of the notochord. It is expressed at low levels in the hindgut, except for the cranial half of the cloaca (where the level of expression is very high) and in the most caudal part (where there is no detectable signal) (Fig. 2A). The caudal border of expression in the floorplate of the neural tube is immediately dorsal to the cranial part of the cloaca (arrow in Fig. 2A). On the sections (Fig. 3), examined in caudal to cranial sequence, *Shh* expression is first detected in the notochord when this structure is morphologically clearly defined (section c); it extends cranially along the notochord with a greater level of expression in the central cells than in the peripheral ones. The sections also show that the high level of signal in the gut epithelium is confined to the lateral and ventral regions, being low or absent from the dorsal cells close to the notochord (section e). The first signal within the neuroepithelium is observed in a few ventral cells at the tip of the V-shaped neural tube, just cranial to section e (not shown).

HNF3α. In the most caudal part of the embryos, clear expression of *HNF3*α is present only in the notochord (Fig. 2B). A weak and patchy expression is observed in the caudal end of the hindgut, concentrated on the apical aspect of the epithelium, but a strong signal is confined to the cranial part of the dilated cloacal region. This coincides with the region showing strong *Shh* expression and also resembles *Shh* in having lower expression close to the notochord (Fig. 3, section e). However, unlike *Shh*, a very strong *HNF3*α signal is continuous along the gut cranial to the cloaca (Fig. 2B). A weak signal is detected in the apical region of the neuroepithelium, although this is barely detectable in the more caudal neural tube (Fig. 3, sections c,d). In one of three embryos examined after sectioning, a weak signal was detectable in a few cells of the floorplate. In the other two embryos no labelling could be detected, the caudal border probably being located cranial to section e on Figure 3 (arrow in Fig. 2B). Expression in the most caudal part of the notochord is apparent before a cord structure is clearly formed (Fig. 3, section b). Cranial to that level, *HNF3*β is expressed all along the notochord.

HNF3β. Expression of *HNF3*β is observed in the notochord, hindgut, and floorplate of the neural tube (Fig. 2C). In the notochord and hindgut, the expression domain extends to the caudal extremities of these structures, in contrast to the neural tube, in which the caudal border of expression is located at the level of ventral curvature, above the caudal part of the cloaca (arrow in Fig. 2C). Analysis of sections revealed expression in prenotochordal axial cells before they compact into a cord (Fig. 3, section b). Cranial to that level, *HNF3*β is strongly expressed in the notochord, becoming weaker as expression in the floorplate is increased (section e). Expression in the hindgut is strongest dorsally and weakest ventrally (sections c-d). In the dorsal region, the signal is stronger where the notochord has most recently formed as a definitive structure and becomes weaker where floorplate expression is strong (section e). At these levels the staining is concentrated on the apical (luminal) aspect of the gut epithelial cells. The first signal in the neuroepithelium is observed at approximately 500 μm from the tip of the tail in just four to five cells located in the floorplate (section d). At that level, the neural tube is closed and has a clear V-shaped ventral aspect. This signal increases progressively in intensity and extends lateral to the floorplate in progressively more cranial sections.

Wnt5b. *Wnt5b* is expressed at a high level in the most caudal part of the embryo. The tissues involved are the central/dorsal tail bud mesenchyme, the caudal neuropore, and the caudal extremity of the hindgut (Figs. 2D, 3, section a,b). Expression in the neuropore and recently closed neural tube decreases markedly in the cranial direction, ending after four to five sections (250 μm). Expression of *Wnt5b* is observed in notochordal cells and the hindgut as they begin to differentiate (Fig. 3, sections b,c), but the staining is apparent on only three or four sections (200 μm).

Evx1. *Evx1* is expressed at a high level in the tail bud mesenchyme and at the caudal end of the neural tube, including the tissue surrounding the neuropore (Fig. 2E). At the level of the ventral curvature of the tail, a diffuse domain of expression is observed in the ventromedial mesenchyme, adjacent to the VEG (arrow in Fig. 2E). In the hindgut, expression is concentrated in the apical part of the cells, except for the most caudal region. A very high level of expression is observed in the open neuroepithelium of the caudal neuropore and in the recently closed neural tube (Fig. 3, sections b,c). The intensity decreases in the cranial direction, beginning in the roof of the neural tube where no more transcripts are detected after apposition of the neural folds (Fig. 3, section c).

RARγ. *RAR*γ is expressed at a low level in all tissues of the tail region, including the surface ectoderm, with a caudal border located just cranially to the most recently formed somite. Within this caudal domain, there are differential levels of expression (Fig. 2F). In the tail bud, central and dorsal cells show higher levels than the ventral/peripheral ones, especially at its cranial end, where neural plate and notochord begins to differentiate. This high level of expression is maintained within epiblast and the neural plate of the open neuropore. The intensity of expression first decreases moderately caudocranially along the neuropore, then decreases sharply in the closed neural tube, to be undetectable at the level of the somites. Within the mesoderm, the ventral midline area above the VER is

more strongly labelled than the lateral and paraxial regions (Fig. 3, sections b,c). In progressively more cranial sections, there is a downregulation of the expression in the paraxial mesoderm, concomitant with an increase and extension of the expression in the ventral area. Where the paraxial cells condense to form an epithelial somite, expression is undetectable in the paraxial mesoderm (section d). More cranially, only the mesenchyme of the hindlimb buds shows strong staining (not shown). The surface ectoderm is labelled at a low level except for the VER, in which transcripts are undetectable although its adjacent mesenchyme is labelled (arrow in Fig. 3, section b). In older embryos, following closure of the neuropore, the most intense domain of expression becomes progressively restricted to the tail bud.

Wnt5a. A high level of expression is observed in the tail bud, the PNP region, and extending cranially to a poorly defined border located at the level of ventral curvature (Fig. 2G). The cranial border of expression is in the paraxial mesoderm condensing to form the last somite (arrow in Fig. 2G). All tissues adjacent to the tail bud, except the notochord, show expression of *Wnt5a* (Fig. 3, section b). Surface ectoderm expression is confined to the VER (arrow in Fig. 3). In the open neural plate and recently closed neural tube, the signal is very strong dorsolaterally (sections b-c). Cranial to this level, neuroepithelial expression becomes confined to the apical region and is progressively downregulated (sections d-e). Except for the most caudal part of the gut, expression in the hindgut epithelium is concentrated in the apical part of the cells. The pattern of expression in the mesoderm is very dynamic. Beneath the neuropore, a high level of expression is observed in ventral and lateral regions; ventral cells located just above the VER show the most intense labelling (section b). The signal intensity of the ventral mesenchyme decreases cranially, concomitantly increasing dorsolaterally, being particularly strong in the future dermomyotome (section d). The main feature of the *Wnt5a* pattern is the very high level of expression observed in the VER and adjacent mesenchyme (section b); this expression progressively decreases cranially, with transcripts being undetectable in the VEG (section d).

Brachyury. Very strong expression of *Brachyury* is observed in tail bud, epiblast, gastrulating mesoderm, and the most caudal hindgut (Fig. 2H). In the tail bud and where the caudal neuropore is open, only the surface ectoderm is unlabelled (Fig. 3, section b). Cranial to the neuropore, only the notochord maintains a high level of expression. Within the neuropore, the actively curving neuroepithelium shows a high and uniform level of expression; in the closed neural tube, just before extinction of the signal, the labelling seems to be more intense in the median and lateral hinge points (Fig. 3, section d). The mesenchymal expression domain becomes progressively restricted to the dorsal paraxial mesenchyme, being lost before condensation of the most recently formed somite.

Hoxb1. *Hoxb1* shows a high level of expression in the tail bud, the primitive streak, and primary mesenchyme (Fig. 2I). The cranial border of the mesenchymal domain is located at the ventral curvature, with a ventral to dorsal restriction of the domain in progressively cranial sections. It is present in the condensing somites, particularly in the future dermomyotome (Fig. 3, section d), but is downregulated in complete somites (section e). Similarly, expression in the apical neuroepithelium becomes restricted to the dorsal half of the tube in the most cranial sections (section e). Expression was not observed in the surface ectoderm or in the hindgut. Only the most recently formed (caudal) notochord is labelled.

Fgf8. *Fgf8* is expressed in a very small area at the tip of the tail, including the dorsal half of the tail bud, the neural plate/tube, the condensing prenotochordal cells, and the caudal end of the hindgut (Fig. 2J, Fig. 3 sections a–c). The border of expression is just cranial to the neuropore, except for the dorsal hindgut epithelium, in which a signal is observed slightly more cranially. A high level of expression is present in the epiblast and neural plate. Where the neural tube is closed, the expression is absent from the roofplate (Fig. 3, section b); cranial to this level, it is strongest at the median and lateral hinge points. A low and diffuse staining is observed in all mesenchyme of the tail bud and adjacent sections, being lost in a ventral to dorsal sequence in progressively more cranial sections, beginning at the level of the VEG (Fig. 3, section c).

Cell Proliferation Patterns in the Developing Tail

Regional analysis of cell proliferation within the tail bud, caudal mesoderm, and VER was performed by means of 5-Bromo-2′-deoxyuridine (BrdU) uptake and immunohistochemical detection. Uniform cell proliferation is evident within the tail bud (Fig. 5a). The distribution of BrdU-labelled cells in the caudal mesoderm revealed four domains, delineated by both transverse and craniocaudal boundaries, which differ in their rate of cell proliferation. A subectodermal domain of rapid cell proliferation was evident at all levels cranial to the tail bud (Fig. 5b–d), whereas the paraxial, ventrolateral, and ventromedial mesodermal domains demonstrated more complex, dynamic patterns during tail growth, requiring quantitative analysis (Table 1). At the most caudal level adjacent to the tail bud (Fig. 5b), cell proliferation appears homogeneous throughout the mesoderm below the newly formed neural plate. At the level of the recently closed neural tube (Fig. 5c), the ventromedial mesoderm maintains a uniform rate of proliferation while a fraction of BrdU-labelled cells progressively diminishes within the ventrolateral and paraxial domains, leading to a ventrodorsal gradient of proliferation (Table 1). At the most cranial level ana-

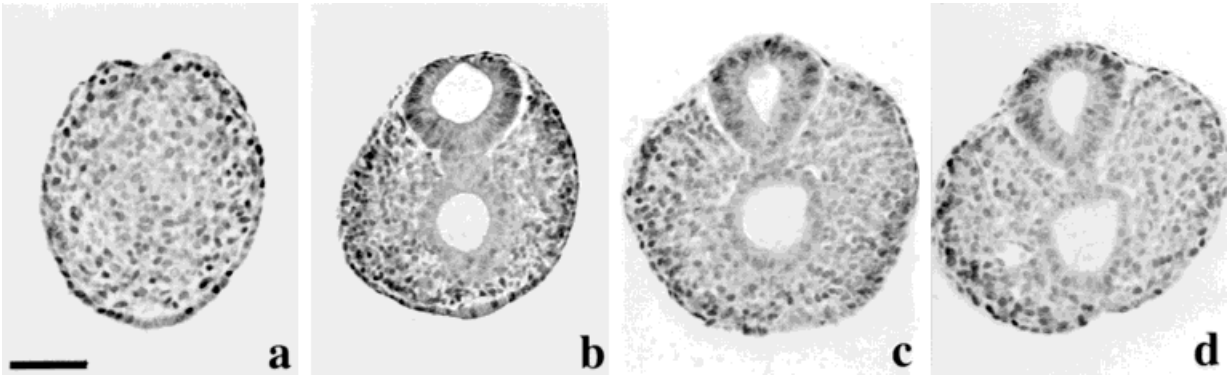

Fig. 5. Immunocytochemistry for BrdU on transverse sections of tails (10 µm). Intensively stained nuclei are those that incorporated BrdU during S-phase. Sections are presented in a caudal to cranial sequence (**a–d**), each section being approximately 200 µm cranial to the previous one. Scale bar = 250 µm

TABLE 1. Quantitative Analysis of Cell Proliferation in the Developing Tail[a]

	Level b	Level c	Level d
Paraxial mesoderm	0.56 ± 0.06[1]	0.50 ± 0.06[1,2]	0.49 ± 0.05[4,5]
Ventrolateral mesoderm	0.55 ± 0.05	0.53 ± 0.06[3]	0.56 ± 0.07[4]
Ventromedial mesoderm	0.55 ± 0.05	0.58 ± 0.09[2,3]	0.56 ± 0.06[5]
VER/VEG	0.42 ± 0.13[6]	0.32 ± 0.08[7]	0.22 ± 0.08[6,7]

[a]Values are as means ± standard deviation, calculated using 20–27 samples in each case. The different levels analysed (levels b to d) refer to section levels defined in Figure 1 and illustrated in Figure 5. Superscript numbers indicate statistically significant differences in the independent Student's t-test ($P = 0.05$) between the two data sets.

lysed (Fig. 5d), the caudal mesoderm becomes clearly divided into two domains: a rapidly proliferating ventrolateral domain and a significantly less active paraxial domain (Table 1).

Quantitative analysis of cell proliferation within the VER and VEG was also performed. This demonstrated a high rate of cell proliferation within the VER, which significantly decreases at more cranial levels as the transformation to VEG occurs (Table 1).

DISCUSSION

We have analysed the expression patterns of 10 genes known to be involved in gastrulation and/or early neurulation in the PNP region of early day 10 mouse embryos. The time scale of this analysis was very short, spreading over 6 somite stages (approximately 12 hr) and covering the period of transition from primary to secondary neurulation and axis formation. All genes were found to be expressed in one or more tissues of the tail; significantly, some of them showed a clear time-dependent evolution of their expression patterns over this short period. A summary of the patterns of expression of the 10 selected genes, combining data obtained from 3–9 embryos per gene, is presented in Figure 4 (in which different levels of transcripts are represented by different levels of gray). It is striking that the patterns of expression correlate well with differentiating structures of this region, notably the notochord, hindgut, and neuroepithelium, and define distinct domains within apparently homogeneous structures such as the tail mesenchyme. As shown in Figure 4, there are only a limited number of patterns for each tissue; these are shown schematically in Figure 6, summarised in Table 2, and further discussed below.

Tail Bud

The tail bud consists of a mass of apparently undifferentiated mesenchymal cells covered by surface ectoderm. A recent fate-mapping study of late primitive streak stage mouse embryos using DiI cell labelling showed that posterior epiblast cells continue to gastrulate to form posterior mesoderm as long as the PNP remains open, but not later (Wilson and Beddington, 1996). After PNP closure, caudal structures are formed from the tail bud mesenchyme. This continuity of function from epiblast, primitive streak and node to tail bud is reflected in a continuity of expression of the genes *Wnt5a*, *Wnt5b*, *Evx1*, *RARγ*, *Brachyury*, and *Hoxb1* from the primary axial region to specific patterns within the tail bud. *Brachyury* and *Hoxb1* are expressed throughout the tail bud mesenchyme (Fig. 6, pattern A), whereas *Wnt5b*, *Evx1*, and *RARγ* are expressed preferentially within the dorsal and central tail bud cells, which differentiate to form the neural tube, notochord, and hindgut (Fig. 6, pattern B). *Wnt5a* shows a lower level of expression in the central (presumptive notochordal) cells of the tail bud (Fig. 6, pattern C), consistent with the absence of its expression in the notochord (Fig. 3, sections b–e) and in the

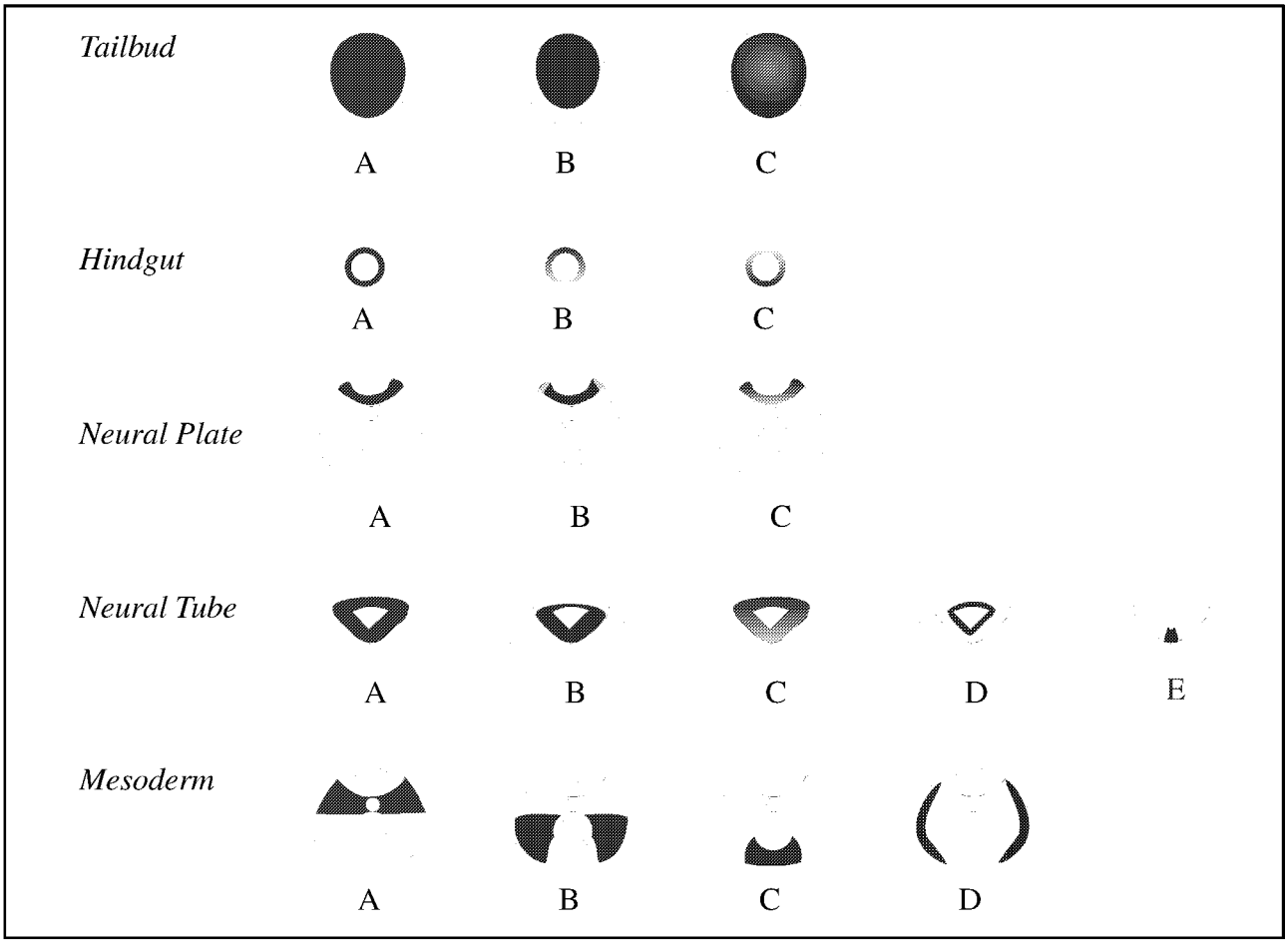

Fig. 6. Schematic representation of patterns observed in the different tissues present in the tail during PNP closure. The letter beneath each pattern links the pattern to the gene expression summary in Table 2. Notochord is not illustrated because expression was either present or not detected (Table 2) without showing a specific pattern.

anterior streak or node during gastrulation (Takada et al., 1994).

Notochord

The main genes involved in induction, formation, and maintenance of the notochord—*HNF3*β, *Shh*, and *Brachyury*—are all present at a high level in the notochordal cells of the tail. Caudocranial analysis reveals that *HNF3*β expression precedes *Shh* in the notochord (Fig. 3). This temporal sequence of expression supports evidence from the respective null mutants, in which *HNF3*β expression is initially required to induce *Shh*, which in turn feeds back to maintain expression of *HNF3*β (Ang and Rossant, 1994; Chiang et al., 1996).

Hindgut

In the mouse, most endodermal cells arise from the epiblast of the anterior primitive streak early in gastrulation (Lawson et al., 1991), with the cells of the dorsal hindgut endoderm being the exception. These cells seem to originate throughout gastrulation at the level of the ventral node, from a population of stem cells that also gives rise to the notochord (Wilson and Beddington, 1996). Formation of the hindgut is initiated by contraction of the proximal yolk sac to form the yolk sac stalk during early somite stages of development. The blind-ended tube elongates as the embryonic trunk grows in length, its caudal extremity underlying the ventral node, until PNP closure. The cloacal membrane is not morphologically distinct at the stage studied here.

Three patterns of expression were evident in the hindgut (Fig. 6). *HNF3*α, *Wnt5b*, *Wnt5a*, and *RAR*γ showed uniform transcript levels in all cells (Fig. 6, pattern A). Dorsal cells expressed higher levels of *HNF3*β, *Brachyury*, and *Fgf8* than ventral cells (Fig. 6, pattern B), whereas *Shh* showed the reverse (Fig. 6, pattern C; Table 1). The specific patterns of expression of *Brachyury* and *Fgf8* may in part reflect the different cell lineage origin of dorsal and ventral endodermal cells during gastrulation. Endodermal induction and

TABLE 2. Summary of Gene Expression in the Tissues Present in the Tail[a]

	Tissues					
Genes	Tail bud	Notochord	Hindgut	Neural plate	Neural tube[b]	Mesoderm[b]
Shh	−	A	C	−	−	−
HNF3α	−	A	A	−	D	−
HNF3β	−	A	B	−	E	−
Wnt5b	B	b-c) A d-e) −	A	A	−	C
Evx1	B	−	A to C	B	B	b-d) C c-e) B + C
RARγ	B	b-d) A e) −	A	A	A	b-c) A + B + C d) B + C (A) e) B + C
Wnt5a	C	−	A	C	C	b) A + B + C + D c-d) D + B, (A, C) e) B
Brachyury	A	A	A to B	A	A to B	b) A + B + C + D c) A + B + D d) A + D e) −
Hoxb1	A	b-c) A d-e) −	−	A	b-c-d) A + D e) C	b) A + B + C + D c) A + B + D d) A e) −
Fgf8	B	b) A c-e) −	A to B	A	B to D	b) A + B C c) A + B d) A e) −

[a]For each tissue, the different patterns of expression observed are represented by capital letters refering to schemes in Figure 6. Notochord expression is either present (A) or not detected (−).
[b]The lower case letters refer to the craniocaudal level of section as defined in Figure 1 and illustrated in Figure 3.

differentiation are thought to involve the *HNF3* genes because their transcripts are present before and during gastrulation in cells fated to be endoderm (Ang et al., 1993). Further evidence comes from the observed upregulation of HNF3 genes during endodermal differentiation of human or mouse embryonal carcinoma cells in culture induced by retinoic acid (Jacob et al., 1994; Roach et al., 1994). Intriguingly, *HNF3*β expression is complementary to that of *Shh*, being highest dorsally, whereas *Shh* is highest ventrally. This reciprocal pattern suggests a different functional interdependence between *HNF3*β and *Shh* in the embryonic hindgut than has been postulated in the more widely studied notochord (see above). Consistent with this interpretation, $Shh^{-/-}$ mutant mice lose late *HNF3*β expression in the notochord while maintaining it in the dorsal hindgut (Chiang et al., 1996). Reciprocally, $HNF3\beta^{-/-}$ mutants maintain *Shh* in the ventral hindgut (Ang and Rossant, 1994).

Neuroepithelium

An extensive morphological study of spinal neurulation in the mouse has shown that until the 25–27 somite stage, closure of the neural tube involves convergence of neural folds via medial and lateral hinge points forming a rhomboid-shaped lumen (Shum and Copp, 1996). In contrast, from the 27 somite stage until the time of closure of the PNP, the caudal neural plate undergoes uniform bending, generating a circular neural tube. This is consistent with our results (Fig. 3) that show that at more cranial levels evidence of hinge points persists, but more caudally the open neural plate assumes a semicircular appearance. However, the neuroepithelial cells in the late neuropore are not uniform in terms of gene expression. Whereas *Wnt5b, RARγ, Brachyury, Hoxb1,* and *Fgf8* are expressed throughout the neural plate, *Evx1* and *Wnt5a* expression reveal distinct cell populations medially, in a domain larger than the future floorplate (Fig. 6, pattern B), and laterally at the tip of the folds (Fig. 6, pattern C). In the closed neural tube these two patterns evolve so that *Evx1* is primarily expressed in the ventral and lateral walls, whereas *Wnt5a* is expressed in dorsal cells forming the roof of the neural tube. The high level of *Wnt5a* expression at the tips of the open neural folds may be functionally related to neural crest cell determination, homologous with the subpopulations of cranial neural crest cell that express *Wnt5a* (Gavin et al., 1990). The transient expression of *Brachyury* throughout the caudal neuroepithelium observed here is in agreement with data reported in chick embryos (Kispert et al., 1995) but different form the described expression of *Xbra* in the roof of the caudal spinal cord in Xenopus embryos (Gont et al., 1993). The functional significance of *Brachyury* expression in the neural tissue is not

known, nor is the explanation of this discrepancy between species.

A striking observation of this study is that the expression of *Wnt5b*, *RARγ*, *Brachyury*, *Hoxb1*, *Fgf8*, *Wnt5a*, and *Evx1* in the open plate is down-regulated once closure of the neural tube is achieved and then further diminishes cranially along the closed neural tube until expression of most of these genes is absent by the level of the most recently formed somites. An important feature of PNP closure is that it defines the point in space and time when gastrulation and primary neurulation cease. The genetic control of this major change at a specific axial level is not understood. An interesting possibility is that one or more of these genes contributes to the termination of primary neurulation and primary body axis formation.

The cells of the floorplate of the recently closed neural tube are specifically labelled by *HNF3β* (Fig. 6, pattern E). This gene has been proposed as a regulator of floorplate development (Sasaki and Hogan, 1994); its induction in the floorplate is regulated by *Shh* from the notochord, mediated by GLI 1 protein (Sasaki et al., 1997). This is consistent with our observation that *HNF3β* expression is initiated in the floorplate slightly cranial to the level of *Shh* expression in the notochord.

Mesoderm

Before the formation of somites, the caudal mesoderm presents a morphologically uniform mesenchymal appearance. With respect to gene expression and cell proliferation, however, the mesoderm is the most complex of the caudal tissues. Four domains were revealed (Fig. 6): (A) paraxial, (B) ventrolateral, (C) ventromedial, and (D) subectodermal. Genes are expressed in one or more of these domains in dynamic patterns according to the axial level (Table 2). The paraxial domain clearly corresponds to the segmental plate. In this domain, expression of *Brachyury*, *Hoxb1*, and *Fgf8* is strong caudally and disappears at a cranial boundary coinciding with early somitic condensation. This is consistent with a role for these genes in the induction and maintenance of undifferentiated embryonic mesoderm before somite formation. Cell proliferation in the paraxial mesoderm also reduces from caudal to cranial, being most active underneath the open neuropore and less active during early somitic condensation. Rapid proliferation of the caudal paraxial mesodermal cells underneath the open neural tube may additionally contribute to elevation of the neural folds.

The ventromedial domain is a small block of tissue adjacent to the tail bud. It lies between the hindgut and the VER and narrows progressively in more cranial sections, with its cranial boundary just caudal to the cloacal membrane. This mesodermal domain has a high rate of cell proliferation and is specifically labelled by probes to *Wnt5a*, *RARγ*, and *Evx1* (Fig. 3). At a more cranial level, the expression of these three genes divides the tail mesoderm into two regions: the paraxial mesoderm expressing high levels of *Wnt5a* and destined for somitogenesis, and the ventrolateral mesoderm, which expresses *RARγ* and *Evx1* and remains undifferentiated and highly proliferative at this stage.

Wnt5a, *Brachyury*, and *Hoxb1* demarcate a subectodermal domain of gene expression in the mesoderm. No obvious embryonic structure derives from the cells of this region, but our observation of BrdU-labelled sections reveals a particularly high level of cell proliferation in the subectodermal domain throughout the tail. These marginally positioned highly proliferative mesenchymal cells may be responsible for circumferential growth of the tail.

Ventral Ectodermal Ridge

The VER is a thickening of the ectoderm present at the ventral surface of the tail bud and tail region immediately cranial to the tail bud (Gajovic and Kostovic-Knezevic, 1995). More cranially it is continuous with a ventral groove (VEG) that ends at the cloacal membrane. Based on morphological evidence, it has been suggested that the VER is analogous to the apical ectodermal ridge (AER) of the limb buds in being a site of epithelial-mesenchymal interaction (Gajovic and Kostovic-Knezevic, 1995). In this study, only *Wnt5a* was observed to be expressed in the VER; this expression did not extend into the VEG. The VER, but not the VEG, is characterised by rapid cell proliferation, corresponding precisely to the pattern of expression of *Wnt5a* in these structures.

Comparison of gene expression domains and cell proliferation patterns suggests that epithelio-mesenchymal interactions between the VER and overlying mesoderm may promote cell proliferation and maintenance of the undifferentiated state of the ventrolateral mesoderm in the distal tail. *Wnt5a* may act as a signalling molecule in this interaction, consistent with its expression in the AER and underlying mesoderm of the limb, where it is thought to participate in the maintenance of cell proliferation in the progress zone (Gavin et al., 1990). Here comparison with the limb bud ends, because the progress zone mediates limb bud outgrowth, and in contrast, the tail does not expand ventrally. Previously, only one gene was reported to be expressed in the VER, *Msx1* (Lyons et al., 1992). It has recently been shown that *Wnt5a* contains homeodomain binding sites for MSX1 protein (Iler and Abate-Shen, 1996). *Msx1* is expressed at other sites of epithelial-mesenchymal interaction (including the AER) in the embryo and is known to be required for maintaining the undifferentiated state of mesenchymal cells. Taken together, these data strongly support the hypothesis that the VER is a signalling center in the ventral tail.

This detailed descriptive study of gene expression patterns in the caudal region of the mouse embryo during the final phase of primary neurulation provides a number of clear correlations with morphogenetic events, such as neuroepithelial morphogenesis and notochordal condensation, as well as with discrete domains of cell proliferation and differentiation within

morphologically homogeneous structures, particularly the mesenchyme. In general, morphogenetic processes in the caudal region are not well understood; the data provided here suggest that functional correlations should be sought with the newly identified mesodermal subdomains and with the distinctive morphological and molecular nature of the VER. This study also forms a descriptive baseline for comparison with gene expression patterns in mutant strains showing defective spinal neurulation. We report elsewhere a comparison with gene expression patterns in the *curly tail* mouse mutant.

EXPERIMENTAL PROCEDURES

Whole Mount In Situ Hybridisation

C57Bl/6 mice were paired for mating overnight, after which females were checked for vaginal plugs. The day of finding the plug was designated as day 0 of gestation. Females were killed by cervical dislocation on early day 10, and the embryos were dissected free of their membranes. The number of somites was counted, and only embryos with 27–32 somites were processed further. Embryos were fixed in 4% paraformaldehyde and processed for whole mount in situ hybridisation as described by Wilkinson (1992). For analysis, tails were isolated from the body by a cut just cranial to the hindlimb buds.

Plasmids and Probes

Plasmids for in situ hybridisation were kindly provided as follows: *Shh*, *Wnt5a*, and *Wnt5b* by A. McMahon; *HNF3*α and *HNF3*β by B. Hogan; *RAR*γ and *Hoxb1* by P. Chambon; *Brachyury* by R. Beddington; *Fgf8* by I. Mason; and *Evx1* by M. Dush and G. Martin. Plasmids were prepared using a Qiagen plasmid maxi kit (Hybaid, UK). Digoxigenin-labelled riboprobes were synthesised from linearised plasmids in a standard T3, T7, or Sp6 polymerase reaction.

Vibratome Sections

After observation and photography, the whole tails were embedded in gloop (egg albumin [57 g], gelatin [0.75 g], and sucrose [30 g] in phosphate buffer 0.1 M, pH 7.3, [150 ml], mixed 10:1 with glutaraldehyde 25%). Freshly embedded specimens were cut on a vibratome at 50 μm. Sections were air-dried and mounted in DPX medium for observation.

Cell Proliferation Analysis

Pregnant CBA/ca mice were given a single intraperitoneal injection of 100 mg/kg body weight of BrdU (Boehringer Mannheim, UK) on early day 10 and killed by cervical dislocation 2 hr later. Embryos were dissected free of their extraembryonic membranes, and the tails were removed by a cut cranial to the hindlimb buds. They were fixed in Bouin's solution overnight, embedded in paraffin wax, and cut transversely at 10 μm. Immunohistochemical detection of incorporated BrdU was performed using mouse anti-BrdU primary antibody (Boehringer Mannheim, UK) and biotinylated goat anti-mouse IgG secondary antibody (Vector Laboratories, UK). Bound antibody was detected by DAB colour reaction with avidin biotin complex (Vector) amplification. Sections were counterstained with Erhlich's hematoxylin before mounting.

For quantitative analysis, three adjacent transverse sections were selected at three points along the caudocranial axis of mouse tails (approximately 200, 400, and 600 μm from the tip of the tail). Cells were counted using an eyepiece graticule at ×400 magnification. The fraction of proliferating cells was calculated as the number of stained cells within a defined mesodermal domain (paraxial mesoderm, ventrolateral mesoderm, and ventral mesoderm) divided by the total number of cells within the same domain. Cell proliferation was analysed in at least 20 separate tails, and the non-paired Student's t-test was used to interpret the data.

ACKNOWLEDGMENTS

The authors thank all members of the GM M-K research group for helpful discussion and comments, in particular Youichirou Ninomiya for his help in preparing figures. This research was supported by grant No. G9421750N from the Medical Research Council and by a Fellowship from the European Molecular Biology Organisation to F.G.; M.H. is currently funded by a Foulkes Foundation Fellowship.

REFERENCES

Ang S-L, Rossant J. HNF-3β is essential for node and notochord formation in mouse development. Cell 1994;78:561–574.

Ang S-L, Wierda A, Wong D, Stevens KA, Cascio S, Rossant J, Zaret KS. The formation and maintenance of the definitive endoderm lineage in the mouse: Involvement of *HNF3/forkhead* proteins. Development 1993;119:1301–1315.

Chiang C, Litingtung Y, Lee E, Young KE, Corden JL, Westphal H, Beachy PA. Cyclopia and defective axial patterning in mice laking *Sonic hedgehog* gene function. Nature 1996;383:407–413.

Dush MK, Martin GR. Analysis of mouse *Evx* genes: *Evx-1* displays graded expression in the primitive streak. Dev. Biol. 1992;151:273–287.

Echelard Y, Epstein DJ, St-Jacques B, Shen L, Mohler J, McMahon JA, McMahon AP. Sonic hedgehog, a member of a family of putative signaling molecules, is implicated in the regulation of CNS polarity. Cell 1993;75:1417–1430.

Faust C, Magnuson T. Genetic control of gastrulation in the mouse. Curr. Opin. Genet. Dev. 1993;3:491–498.

Gajovic S, Kostovic-Knezevic L. Ventral ectodermal ridge and ventral ectodermal groove: Two distinct morphological features in the developing rat embryo tail. Anat. Embryol. 1995;192:181–187.

Gavin J, McMahon JA, McMahon AP. Expression of multiple novel Wnt-1/int-1-related genes during fetal and adult mouse development. Genes Dev. 1990;4:2319–2332.

Gont LK, Steinbeisser H, Blumberg B, De Robertis EM. Tail formation as a continuation of gastrulation: The multiple cell populations of Xenopus tailbud derive for late blastopore lip. Development 1993;119: 991–1004.

Hermann BG. The mouse *Brachyury (T)* gene. Semin. Dev. Biol. 1995;6:385–394.

Iler N, Abate-Shen C. Rapid identification of homeodomain binding

sites in the *Wnt-5a* gene using immunoprecipitation strategy. Biochem. Biophys. Res. Commun. 1996;227:257–265.

Jacob A, Budhiraja S, Qian X, Clevidence D, Costa RH, Reichel RR. Retinoic acid-mediated activation of *HNF3*α during EC stem cell differentiation. Nucleic. Acid Res. 1994;22:2126–2133.

Kispert A, Ortner H, Cooke J, Herrmann BG. The chick *Brachyury* gene: Developmental expression pattern and response to axial induction by localized activin. Dev. Biol. 1995;168:406–415.

Lawson KA, Meneses JJ, Pedersen RA. Clonal analysis of epiblast fate during germ layer formation in the mouse embryo. Development 1991;113:891–911.

Lyons GE, Houzelstein D, Sassoon D, Robert B, Buckingham ME. Multiple sites of Hox-7 expression during mouse embryogenesis: Comparison with retinoic acid receptor mRNA localization. Mol. Reprod. Dev. 1992;32:303–314.

Mahmood R, Bresnick J, Hornbruch A, Mahony C, Morton N, Colquhoun K, Martin P, Lumdsen A, Dickson C, Mason I. A role for FGF-8 in the initiation and maintenance of vertebrate limb bud outgrowth. Curr. Biol. 1995;5:797–806.

Murphy P, Hill RE. Expression of the mouse *labial*-like homeobox-containing genes, *Hox 2.9* and *Hox 1.6*, during segmentation of the hindbrain. Development 1991;111:61–74.

Parr BA, McMahon AP. Wnt genes and vertebrate development. Curr. Opin. Genet. Dev. 1994;4:523–528.

Placzek M. The role of the notochord and floorplate in inductive interactions. Curr. Opin. Genet. Dev. 1995;5:499–506.

Roach S, Schmid W, Pera M. Hepatocytic transcription factor expression in human embryonal carcinoma and yolk sac carcinoma cell lines: Expression of *HNF-3*α in models of early endodermal cell differentiation. Exp. Cell Res. 1994;215:189–198.

Ruberte E, Dollé P, Chambon P, Morriss-Kay GM. Retinoic acid receptors and cellular retinoid binding proteins. II. Their differential pattern of transcription during early morphogenesis in mouse embryos. Development 1991;111:45–60.

Sasaki H, Hogan BLM. *HNF-3*β as a regulator of floor plate development. Cell 1994;76:103–115.

Sasaki H, Hui C-C, Nakafuku M, Kondoh H. A binding site for *Gli* proteins is essential for *HNF3*α floor plate enhancer activity in transgenics and can respond to *Shh in vitro*. Development 1997;124: 1313–1322.

Shum ASW, Copp AJ. Regional differences in morphogenesis of the neuroepithelium suggest multiple mechanisms of spinal neurulation in the mouse. Anat. Embryol. 1996;194:65–73.

Takada S, Stark KL, Shea MJ, Vassileva G, McMahon JA, McMahon AP. Wnt-3a regulates somite and tailbud formation in the mouse embryo. Genes Dev. 1994;8:174–189.

Wilkinson DG. Whole mount *in situ* hybridisation of vertebrate embryos. In: Wilkinson DG, ed. *In Situ* Hybridisation. Oxford: IRL Press, 1992:75–83.

Wilson V, Beddington RSP. Cell fate and morphogenetic movement in the late mouse primitive streak. Mech. Dev. 1996;55:79–89.

Wood HB, May G, Healy L, Enver T, Morriss-Kay GM. (1997) CD34 expression patterns during early mouse development are related to modes of blood vessel formation and reveal additional sites of hematopoiesis. Blood 1997;90:2300–2309.

Yamaguchi TP, Rossant J. Fibroblast growth factors in mammalian development. Curr. Opin. Genet. Dev. 1995;5:485–491.